MOLECULAR AND CELLULAR BIOLOGY, May 2006, p. 3401–3413 Vol. 26, No. 9
0270-7306/06/$08.00+0 doi:10.1128/MCB.26.9.3401–3413.2006
Copyright © 2006, American Society for Microbiology. All Rights Reserved.

The Negative c-Myc Target Onzin Affects Proliferation and Apoptosis via Its Obligate Interaction with Phospholipid Scramblase I†

Youjun Li,[1] Kenneth Rogulski,[1] Quansheng Zhou,[2] Peter J. Sims,[2] and Edward V. Prochownik[1,3,4]*

Section of Hematology/Oncology, Department of Pediatrics, Children's Hospital of Pittsburgh, Pittsburgh, Pennsylvania[1]; Department of Molecular and Experimental Medicine, Scripps Research Institute, La Jolla, California[2]; and Department of Molecular Genetics and Biochemistry, University of Pittsburgh Medical Center,[3] and University of Pittsburgh Cancer Institute,[4] Pittsburgh, Pennsylvania

Received 26 August 2005/Returned for modification 3 October 2005/Accepted 10 February 2006

Onzin, the product of a negatively c-Myc-regulated target gene, is highly expressed in myeloid cells. As a result of its interaction with and activation of Akt1 and Mdm2, onzin down-regulates p53. The apoptotic sensitivity of several cell lines is thus directly related to onzin levels. We have conducted a search for additional onzin-interacting proteins and identified phospholipid scramblase 1 (PLSCR1), an endofacial membrane protein, which is proposed to mediate the bidirectional movement of plasma membrane phospholipids during proliferation and apoptosis. PLSCR1 interacts with the same cysteine-rich domain of onzin as do Akt1 and Mdm2, whereas the onzin-interacting domain of PLSCR1 centers around, but does not require, a previously identified palmitoylation signal. Depletion of endogenous PLSCR1 in myeloid cells leads to a phenotype that mimics that of onzin overexpression, providing evidence that PLSCR1 is a physiologic regulator of onzin. In contrast, PLSCR1 overexpression in fibroblasts, which normally do not express onzin, affects neither growth nor apoptosis unless onzin is coexpressed, in which case PLSCR1 completely abrogates onzin's positive effects on proliferation and survival. These findings demonstrate a functional interdependence between onzin and PLSCR1. They further suggest a contiguous link between the earliest events mediated by c-Myc and the latest ones, which culminate at the cell surface and lead to phospholipid reshuffling and cell death.

Deregulation of the *CMYC* oncogene in human cancers often occurs as a result of gene amplification, chromosomal translocation, mRNA stabilization, or gain-of-function mutations in factors that regulate *CMYC* gene transcription (24). Under these circumstances, and because it serves as a general transcription factor, c-Myc can alter the expression of literally hundreds of target genes regulated by RNA polymerases I, II, and III (1, 10, 13, 15, 16, 25, 35). At the cellular level, the consequences of this global loss of properly coordinated gene expression include increases in cell size and metabolism, enhanced sensitivity to apoptotic stimuli, abnormalities of cell cycle progression, increased proliferation, inhibition of the ability to differentiate, genomic instability, and transformation (reviewed in reference 29). Collectively, these changes in cellular physiology and behavior have been termed the c-Myc phenotype.

One of the challenges confronting the study of c-Myc is to understand which of its diverse transcriptional targets are responsible for imparting each phenotype, particularly that of transformation. Over the past several years, a number of studies have revealed that one or more of these phenotypes can be recapitulated by the overexpression of some polymerase II-regulated c-Myc target genes (26, 29, 37, 40). This has led to the general hypothesis that the complex c-Myc phenotype derives from the interplay among a large number of its downstream target genes, many of which have overlapping or redundant functions.

We have recently characterized a novel negative c-Myc target gene, termed *onzin*, which is highly expressed by myeloid cells (28). The ectopic overexpression of c-Myc leads to a dramatic reduction of endogenous onzin that coincides with the cell's increased susceptibility to a variety of apoptotic stimuli. That onzin's function is directly linked to this phenotype is supported by the observation that its depletion by short hairpin RNA (shRNA) sensitizes cells to these apoptotic insults without altering endogenous c-Myc levels. Furthermore, the enforced expression of onzin in fibroblasts, which normally express little or none of the protein, leads to marked apoptotic resistance, loss of G_2/M checkpoint control, enhanced proliferation, and tumorigenic conversion. These functions require that onzin be able to shuttle between the plasma membrane and nucleus and to interact directly with and activate the Akt1 and Mdm2 oncoproteins. Ultimately, this leads to an inability to up-regulate p53, which, in turn, results in a loss of cell cycle arrest and apoptotic response. The c-Myc–onzin–p53 association thus appears to represent a novel and possibly cell type-specific arm of a previously described pathway by which c-Myc activates the $p19^{ARF}$ tumor suppressor, leading to the inhibition of Mdm2 and the stabilization of p53 (16, 17, 45).

Phospholipid scramblase 1 (PLSCR1) is a 35-kDa endofacial membrane protein that has been proposed to mediate the bidirectional movement of plasma membrane phospholipids in response to high levels of cytosolic calcium, injury, or apoptotic insult (5, 31–33). PLSCR1 interacts with a number of molecules involved in growth factor and cytokine signaling, including the epidermal growth factor receptor, shc, src, and c-Abl (23, 32, 33). Overexpression of PLSCR1 has been reported to

* Corresponding author. Mailing address: Section of Hematology/Oncology, Children's Hospital of Pittsburgh, Room 8124, Rangos Research Center, 3460 Fifth Ave., Pittsburgh, PA 15213. Phone: (412) 692-6795. Fax: (412) 692-5228. E-mail: procev@chp.edu.

† This is paper no. 17685-MEM from the Scripps Research Institute.

inhibit tumorigenesis, to promote apoptosis, and to play a role in facilitating the differentiation of myeloid cells (30, 41, 43). In response to cytokine stimulation, a significant fraction of PLSCR1 is depalmitoylated and traffics to the nucleus, where it can enhance the expression of the inositol 1,4,5-triphosphate receptor type 1 gene by directly binding to its promoter (4, 44).

In order to explore further the mechanism(s) by which onzin mediates its profound effects on proliferation, survival, and transformation, we have conducted a standard yeast two-hybrid screen to identify novel onzin-interacting proteins. We report here that PLSCR1 is one such molecule. Tagging onzin and PLSCR1 with spectral variants of green fluorescent protein (GFP) and coimmunoprecipitation experiments revealed that the two proteins colocalize and directly interact in vivo. shRNA-mediated depletion of endogenous PLSCR1 markedly enhances the growth and survival of myeloid cells that normally express onzin. Conversely, in both primary and established fibroblasts, PLSCR1 overexpression reverses the profound survival and growth advantage imparted by the enforced expression of onzin. Taken together, these studies reinforce the previously proposed role for onzin in the control of proliferation and apoptosis through p53-dependent pathways (28). In addition, the newly described relationship between onzin and PLSCR1 provides a direct link between the proximal transcriptional control of c-Myc target gene expression and more-distal cell surface events associated with apoptosis.

MATERIALS AND METHODS

Yeast two-hybrid screening. Yeast two-hybrid screening was performed as previously described (38). The full-length murine onzin coding sequence was first amplified under standard PCR conditions using the forward primer 5′-CGC CGT CGA CAA ATG GCT CAG GCA CCA ACA G-3′ and the reverse primer 5′-CGC GTC GAC TTA GAA AGC CTT CAT GGC TCT-3′. The amplified product was agarose gel purified, digested with SalI, and cloned into the pGBK-T7 "bait" vector (Matchmaker Gal4 Two-Hybrid system 3; BD Biosciences-Clontech, San Diego, CA). That the insert was in the correct orientation and in-frame with the vector-encoded Gal4 DNA binding domain and Myc epitope tag was confirmed by DNA sequencing. The vector, which also encodes a yeast *TRP1* gene, was then transformed into *Saccharomyces cerevisiae* AH109. Trp prototrophs were selected, and expression of the fusion protein of the predicted size was verified by immunoblotting of yeast lysates using a monoclonal antibody (MAb) against the Myc epitope tag (9E10; Santa Cruz Biotechnology Inc., Santa Cruz, CA). The yeast cells were then used for high-stringency screening of an 11-day murine fetal cDNA library cloned in the pGAD vector, which also encodes the *LEU2* gene (BD BioSciences-Clontech). In this vector, all open reading frames are fused with a plasmid-encoded hemagglutinin (HA) tag. Transformed yeast cells were plated onto SD/−Leu/−Trp/−Ade/−His (quadruple-knockout) plates.

The total number of colonies screened was determined by plating an aliquot of the transformation mixture onto SD/−Leu/−Trp plates. Colonies arising under the former conditions were then individually picked, regridded onto quadruple-knockout plates, and tested in a filter assay for β-galactosidase expression (20). pGAD plasmids from positive colonies were then isolated in *Escherichia coli*, retransformed individually into the AH109-pGBKT7-onzin yeast strain, selected on quadruple-knockout plates, and again tested for β-galactosidase. Clones remaining positive after this second round of screening were sequenced using a universal pGAD primer in order to identify the cDNA insert. Quantitative β-galactosidase assays were performed on yeast cells grown in liquid culture as previously described (20).

All subsequent experiments with PLSCR1 were performed with the human ortholog in the pGAD-T7 vector such that all expressed proteins were also tagged with the HA epitope. Deletion mutations were obtained by PCR amplification using forward primers containing engineered EcoRI sites and reverse primers containing BamHI sites so as to allow for directional and in-frame cloning into the pGADT7 vector. The expression of all relevant binding domain and activation domain fusion proteins was confirmed by immunoblotting (21) using the Myc epitope tag MAb described above or an anti-HA tag MAb (6E2; Cell Signaling Technology, Beverly. MA), respectively.

All oligonucleotides were synthesized by IDT, Inc. (Coralville, IA).

Plasmids and transfections. To express PLSCR1 as an enhanced yellow fluorescent protein (EYFP) fusion protein, the entire human PLSCR1 coding sequence was PCR amplified with the forward primer 5′-CGC CTC GAG ATC ATG GAA AAC CAC AGC AAG C-3′ and the reverse primer 5′-CGC GTC GAC CTG CCA TGC TCC TGA TCT TTG-3′. Following gel purification and digestion with XhoI and Sal, the fragment was cloned into the SalI-digested pEYFP-C1 vector (BD Biosciences-Clontech). The correct sequence and reading frame were verified by restriction mapping and DNA sequencing and by demonstrating the expression of an appropriately sized, ca. 66-kDa EYFP-PLSCR1 fusion protein by immunoblotting using an anti-GFP MAb (8362-1; BD BioSciences-Clontech). An enhanced blue fluorescent protein (EBFP)-onzin fusion protein was constructed as previously described (28) and produced the predicted 44-kDa protein, as determined by immunoblotting (not shown).

The pSVL-puroMT-onzin vector and the pBABE-IRES-GFP-MT-onzin vector, both of which express full-length, Myc epitope-tagged onzin, have been previously described (28). The latter vector was packaged in the Phoenix-A cell line (28).

Full-length PLSCR1 and its deletion mutants were expressed in the pCMV-FLAG2 or pSVL-neoMT vector as N-terminally Flag or Myc epitope-tagged proteins, respectively. The primers described above for the construction of the EYFP-PLSCR1 fusion protein were used toward this end.

The introduction of specific mutations into both onzin and PLSCR1 was performed with a QuikChange in vitro mutagenesis kit (Stratagene, Inc., La Jolla, CA) according to the directions of the supplier. All mutations were confirmed by DNA sequencing.

To knock down expression of endogenous PLSCR1 in 32D cells, a 65-bp oligonucleotide that contained the target PLSCR1 target sequence 5′-ACC ACA GCA AGC AAA CTG A-3′ and its inverted repeat derived from nucleotides 136 to 154 of the murine PLSCR cDNA sequence (GenBank accession no. AF159593) was designed. The oligonucleotide also contained BamHI and HindIII overhangs to facilitate cloning and a 9-bp "loop" segment and was otherwise designed according to the recommendations of the pSilencer 2.1-U6-puro expression vector supplier (Ambion, Austin, TX). After cloning into this vector, the entire insert was sequenced and then tested in transient-transfection assays with a PLSCR1 murine expression vector to ensure that it successfully reduced protein expression. The linearized vector was then electroporated into 32D cells. Puromycin-resistant cells were then cloned by limiting dilution and expanded for further study.

Cell culture and transfections. 32D murine myeloid cells were cultured in RPMI medium supplemented with 10% fetal calf serum and 10% conditioned medium from the interleukin-3 (IL-3)-producing cell line WEHI-3B as previously described (25). Rat1a, Cos7, and NIH 3T3 cells were cultured in Dulbecco's modified Eagle's medium supplemented with 10% fetal calf serum. Cell culture media were also supplemented with 2 mM glutamine, 100 μg/ml streptomycin, and 100 U/ml penicillin G. Tissue culture media and additives were supplied by Invitrogen (Carlsbad, CA).

Transient transfections were performed using Lipofectamine (Invitrogen) as previously described (28). Stable transfections were performed using Lipofectamine or by electroporation using linearized plasmid DNAs as previously described (22). Antibiotic selections in all cases consisted of either G-418 (500 μg/ml) or puromycin (1 μg/ml). Single-cell-derived individual colonies of transfected Rat1a cells were picked and expanded. Stable 32D transfectants were pooled unless otherwise stated. In all cases of single-cell clones, at least six clones of each cell type were characterized in preliminary experiments. Three clones of each type showing the full range of behaviors are reported here.

Proliferation and apoptosis assays and cell cycle determinations. Growth curves were calculated as previously described (19, 28). For apoptosis assays, logarithmically growing cells were deprived of serum or IL-3 or were treated with the indicated doses of adriamycin, etoposide, or 6-thioguanine (Sigma-Aldrich, St. Louis, MO) as previously described (25, 28). Briefly, in the case of 32D cells, logarithmically growing cells of >90% viability were plated into 12-well plates at a density of 2×10^5 cell/ml in a total volume of 2 ml. The total cell number/well was then determined daily with a Vi-Cell apparatus (Beckman-Coulter Instruments, Miami, FL) as previously described (29). Rat1a cells (>90% viable) were seeded in six-well plates at a density of 2×10^5 cell/plate and allowed to reach approximately 50% confluence. Cells were subsequently trypsinized from triplicate plates, and the total number of wells/plate was determined as described above. A minimum of 2,000 cells per time point were examined. That cell death was occurring by apoptosis was confirmed in select instances by terminal deoxynucleotidyltransferase-mediated dUTP-biotin nick end labeling (TUNEL) assays or by

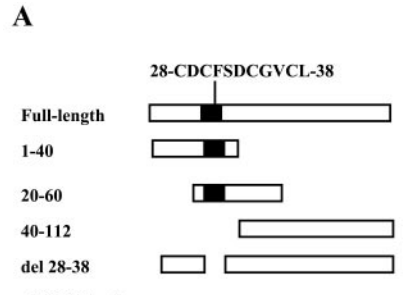

Growth on His⁻ Ade⁻ medium		Relative β-galactosidase activity	
PLSCR1	pGADT7	PLSCR1	pGADT7
+	-	1	≤0.05
+	-	1.39	≤0.05
+	-	2.5	≤0.05
-	-	≤0.05	≤0.05
-	-	≤0.05	≤0.05
-	-	≤0.05	≤0.05

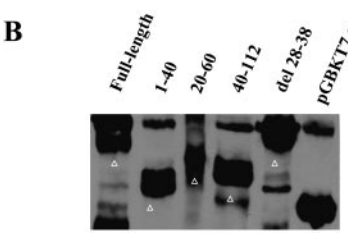

FIG. 1. Identification of the PLSCR1-interacting domain of onzin. (A) The cartoon shows the deletion mutants of murine onzin that were expressed as Gal4 DNA-binding domain fusion proteins in the pGBK-T7 vector. The critical PLSCR1-interacting domain residing between amino acids 28 and 38 is indicated by the black box, with the actual sequence displayed above the depiction of the full-length molecule. The table summarizes the ability of yeast cells expressing each of these mutants and coexpressing either a Gal4 activation domain-PLSCR1 fusion or the activation domain alone (e.g., the empty pGADT7 vector) to grow on medium lacking histidine and adenine and to express β-galactosidase. Each β-galactosidase assay was performed in triplicate on several occasions, and the results of a typical assay are shown, with the activity of the full-length onzin-PLSCR1 interaction normalized to 1. In all cases standard errors were <5% (not shown). To perform β-galactosidase assays on yeast cells expressing onzin mutants which did not confer Ade^+ His^+ prototrophy, these nutrients were included in the growth medium. (B) Western blots showing the expression of the indicated Gal4 DNA-binding domain-onzin fusion molecules. We analyzed 50 μg of protein from total yeast lysates in each case (21). Fusion proteins were detected with an MAb directed against a short Myc epitope residing between the binding domain and onzin moieties. The positions of the fusion proteins are indicated by arrowheads. Note that despite a somewhat lower level of fusion protein in lane 3, this yeast strain expressed the highest levels of β-galactosidase.

determination of subdiploid DNA content using flow cytometry as previously described (19, 38–40).

Protein detection and interactions. Fluorescence microscopy of Cos7 cells transiently transfected with EYFP-PLSCR1 and EBFP-onzin was performed as previously described (28, 29). Briefly, cells were fixed in paraformaldehyde approximately 10 h after Lipofectamine-mediated transfection. GFP fluorescence was observed with an Olympus Provis visual optical system using Magnafire digital imaging software (Olympus America, Melville, NY) outfitted with a triple-pass filter (Chroma Technology Corp., Rockingham, VT).

Coimmunoprecipitation experiments with transiently transfected Cos7 or Rat1a cells were performed essentially as described previously (22). Briefly, confluent monolayers were washed three times in phosphate-buffered saline, collected by scraping, washed an additional three times in phosphate-buffered saline, and resuspended in 150 mM NaCl, 50 mM Tris-HCl (pH 8.0), 1 mM EDTA, and 0.5% NP-40 containing a protease inhibitor cocktail (Roche Diagnostics, Indianapolis, IN). After 10 min on ice the cells were disrupted by a 30-second pulse with the microtip of a Branson sonifier at a setting of 7 and then cleared by centrifugation at 10,000 × *g* for 5 min, and 500 μg of the cleared lysate was then incubated for 2 h at 4°C with 10 μl of control rabbit serum followed by 50 μl of protein G-agarose (Affigel; Bio-Rad, Hercules, CA). Depending upon the experiment, the blocked supernatant was then incubated with a 1:1,000 dilution of an anti-Flag MAb (200471; Stratagene) or an anti-PLSCR1 MAb (12). As a control, an equivalent amount of each lysate was incubated with a nonspecific MAb.

Immune complexes were precipitated by the addition of 50 μl of protein G-agarose for 2 h at 4°C. After extensive washing, the complexes were resuspended in 50 μl of sodium dodecyl sulfate-polyacrylamide gel electrophoresis lysis buffer, boiled, and resolved by sodium dodecyl sulfate-12% polyacrylamide gel electrophoresis. Transfer to polyvinylidene difluoride membranes and probing with the anti-Myc epitope MAb (1:1,000) was then performed as previously described (28). The blot was then incubated with a 1:10,000 dilution of the secondary, horseradish peroxidase-coupled rabbit anti-mouse immunoglobulin G (IgG), washed, and subjected to chemiluminescence detection as previously described (28).

RESULTS

PLSCR1 interacts with onzin in a yeast two-hybrid assay. A standard yeast two-hybrid screen was used to identify onzin-interacting proteins. The "bait" vector consisted of the entire coding sequence for the 112-amino-acid murine onzin protein fused in-frame at its N terminus with the yeast Gal4 DNA-binding domain and a Myc epitope tag. Following transformation of the AH109 yeast strain, we screened an 11-day murine fetal cDNA library in the pGADT7 vector, which expresses proteins as fusions with the yeast Gal4 transcriptional activation domain and an HA epitope tag. Clones containing cDNAs encoding proteins potentially capable of interacting with onzin were identified by their ability to confer histidine and adenine prototrophy and strong β-galactosidase expression on the yeast strain.

Out of 10^6 individual cDNAs screened, a total of 36 met these criteria. Following the isolation of each pGADT7 plasmid in *E. coli*, the ability of each to confer the same phenotype on yeast was confirmed by repeat cotransformation with pGBKT7-onzin. The identities of the cDNAs from 16 of these clones were then determined by automated DNA sequencing and BLAST searches, which showed that two of the sequences encoded in-frame fusions with PLSCR1.

Having confirmed that PLSCR1 recurrently registered as an onzin-interacting protein, we next identified the region of onzin that was responsible for this association. To this end, we created several onzin deletion mutants in the pGBK-T7 vector

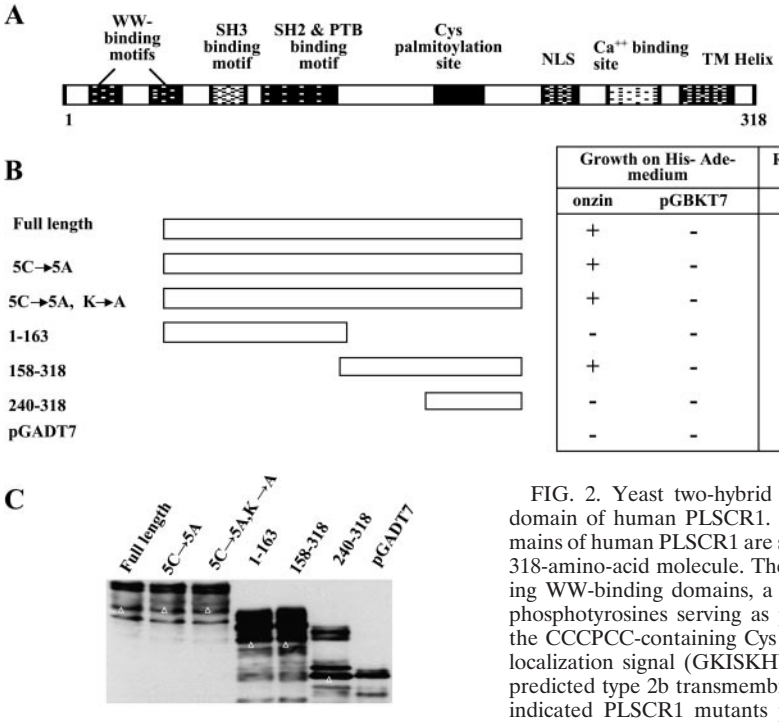

Growth on His- Ade- medium		Relative β-galactosidase activity	
onzin	pGBKT7	onzin	pGBKT7
+	-	1	≤0.05
+	-	0.71	≤0.05
+	-	0.78	≤0.05
-	-	≤0.05	≤0.05
+	-	1.22	≤0.05
-	-	0.22	≤0.05
-	-	≤0.05	≤0.05

FIG. 2. Yeast two-hybrid analysis identifies the onzin-interacting domain of human PLSCR1. (A) Previously identified functional domains of human PLSCR1 are shown on the depiction of the full-length, 318-amino-acid molecule. These domains include two PPXY-containing WW-binding domains, a PXXP-containing SH3-binding domain, phosphotyrosines serving as putative SH2- and PTB-binding motifs, the CCCPCC-containing Cys palmitoylation site, the atypical nuclear localization signal (GKISKHWTGI), the Ca^{2+} binding site, and the predicted type 2b transmembrane (TM) helix (4, 36). (B) Each of the indicated PLSCR1 mutants plus the pGAD vector containing full-length PLSCR1 and the empty pGAD-T7 parental vector was expressed in the AH109-pGBKT7-onzin yeast strain. In the 5C→5A PLSCR1 mutant, the palmitoylation signal CCCPCC was altered to AAAPAA (36). The 5C→5A/K→A mutation contains the palmitoylation site mutation plus mutation K258→A within the nuclear localization signal, which abrogates nuclear trafficking of the protein (4). The table shows the results of yeast growth assays on quadruple-knockout plates and of quantitative β-galactosidase assays as described in the legend to Fig. 1. (C) Expression of human activation domain-PLSCR1 fusion proteins. Western blotting was performed as described for Fig. 1 but were probed with an MAb against the HA tag, located between the activation domain and PLSCR1 moieties. Arrowheads indicate the positions of the fusions proteins.

(Fig. 1A) and showed that each was expressed in yeast at levels nearly identical to those of the wild-type protein (Fig. 1B). The ability of these mutants to confer histidine and adenine prototrophy and β-galactosidase expression was then assessed in the pGADT7-PLSCR1-expressing AH109 yeast strain. As a negative control, the empty pGADT7 vector was used.

As shown in Fig. 1A, full-length human PLSCR1 interacted strongly with the onzin bait, confirming the cross-species specificity of the interaction. Testing of each of the mutants showed that their ability to interact with PLSCR1 was dependent upon the presence an 11-amino-acid, cysteine-rich region between amino acids 28 and 38. This is part of a larger cysteine-rich domain that extends up to amino acid 61 of onzin and contains several CXXC motifs. These, like zinc and RING fingers, also coordinate zinc atoms and are believed to be involved in the catalysis of redox reactions by thiol:disulfide oxidoreductases and in the maintenance of protein conformation and protein-protein interactions (6, 8, 9, 11, 14). From these experiments, we conclude that onzin interacts with PLSCR1 through a specific domain in the former protein whose minimal functional size is 11 amino acids.

The human and murine PLSCR1s are proteins of 318 and 328 amino acids, respectively, that distribute between the plasma membrane and the nucleus. PLSCR1 contains a number of previously mapped functional domains, including a WW- binding motif, a cysteine-rich palmitoylation site, an atypical nuclear localization signal (NLS), a Ca^{2+} binding domain, and a predicted type 2b transmembrane helix (Fig. 2A) (4, 7, 36, 42). In order to determine which, if any, of these motifs was necessary for the interaction with onzin, we used a series of previously characterized or newly derived human PLSCR1 mutants, all of which were expressed in the pGAD-T7 yeast vector (Fig. 2B). Each of these was transformed into the AH109 yeast strain expressing the previously described full-length onzin bait and shown to be expressed at similar levels (Fig. 2C). The full-length human PLSCR1 positive control once again imparted histidine and adenine prototrophy and the expression of high levels of β-galactosidase. Neither a functional palmitoylation site (amino acids 184 to 189) nor an NLS (amino acids 257 to 266) was required for the interaction with onzin, since point mutations within these domains (4, 36) still allowed the expression of a relatively strong His^+ Ade^+ β-galactosidase-positive phenotype (Fig. 2B).

Deletion mutants showed that virtually all of the interaction with onzin occurred via the C-terminal half of PLSCR1 (amino acids 158 to 318), whereas a shorter deletion (amino acids 240 to 318) was inactive. From these experiments, we conclude that the onzin-interacting region of PLSCR1 resides within a domain of the molecule containing residues from ca. 158 to 240 but does not require the Cys palmitoylation site which lies within this region. Unfortunately, we were unable to confirm directly the ability of onzin to interact in yeast with this minimal domain of PLSCR1, as it activated β-galactosidase when expressed as an activation domain fusion protein (not shown).

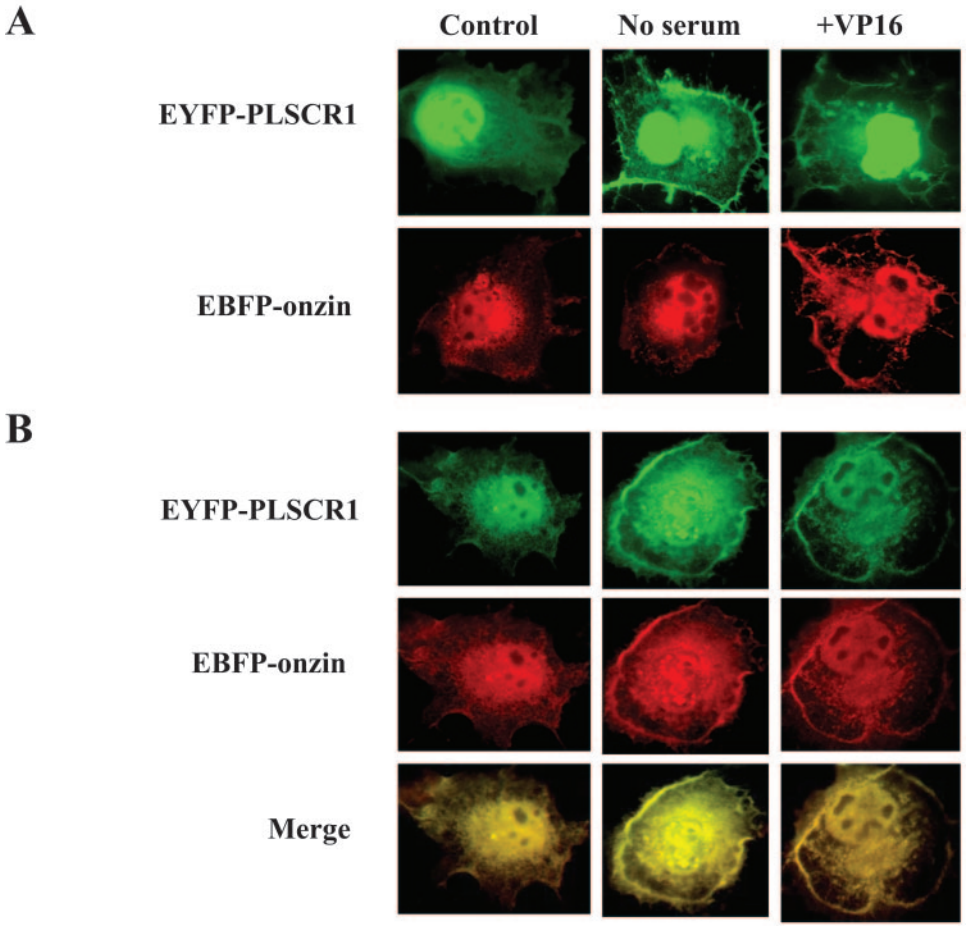

FIG. 3. Expression and colocalization of onzin and PLSCR1 in mammalian cells. (A) Full-length murine PLSCR1 was expressed as an N-terminal fusion with the enhanced yellow fluorescent protein analog of GFP (EYFP) and full-length murine onzin was similarly fused to the enhanced blue variant (EBFP). Each fusion protein was then expressed individually in Cos7 cells, which were fixed 16 h later and viewed by fluorescence microscopy. In columns 2 and 3, cells were deprived of serum or exposed to 125 nM etoposide for 12 h prior to fixation. Typical images are shown. In other experiments, properly sized proteins representing the fusions were observed in the same cells by immunoblotting using an MAb against GFP (not shown). (B) The two proteins were coexpressed, and their individual subcellular localizations were determined by imaging each one singly (28). The bottom row shows the merged images. All of the images depicted here are representative of the appearance of >200 transfected cells.

Direct physical association between onzin and PLSCR1 in mammalian cells. In order to confirm and extend to mammalian cells the above-described interaction between PLSCR1 and onzin, we generated N-terminally tagged fusions with the EYFP or EBFP spectral variant of GFP. In preliminary transient-transfection experiments, we verified by immunoblotting that both EYFP-PLSCR1 and EBFP-onzin were expressed as proteins of the predicted sizes (not shown). We next determined the subcellular location of each protein by direct fluorescence microscopy. As shown in Fig. 3A, both fusion proteins showed mostly nuclear and cytoplasmic patterns. In cells deprived of serum or exposed to the cytotoxic agent etoposide, a more distinct localization of both proteins to the plasma membrane was seen. These findings confirmed our previous observations with onzin (28).

In subsequent experiments, the two proteins were coexpressed under each of the above-described conditions (Fig. 3B). As before, predominantly nuclear and cytoplasmic localization was observed for each in logarithmically growing cells, whereas marked plasma membrane localization was seen under apoptotic conditions. Irrespective of the conditions under which the cells were propagated, however, both proteins strongly colocalized. Together with the results of the yeast two-hybrid experiments (Fig. 1), these studies supported the idea that onzin and PLSCR1 directly interacted.

To provide additional and independent evidence for the onzin-PLSCR1 interaction, Myc epitope-tagged onzin and Flag epitope-tagged PLSCR1 were transiently coexpressed in Cos7 cells. In addition, we also expressed the del28-38 mutant of onzin, which lacks the ability to interact with PLSCR1 in yeast (Fig. 1). After first demonstrating that both onzin proteins were expressed at nearly equivalent levels (Fig. 4A), we performed coimmunoprecipitation experiments using an anti-Flag MAb to precipitate PLSCR1. Immunoblotting was then performed on the precipitates using an anti-Myc epitope tag MAb. As shown in Fig. 4B, full-length onzin but not the del28-38 mutant protein was specifically precipitated from cells coexpressing PLSCR1 (compare lanes 1 and 3). That the im-

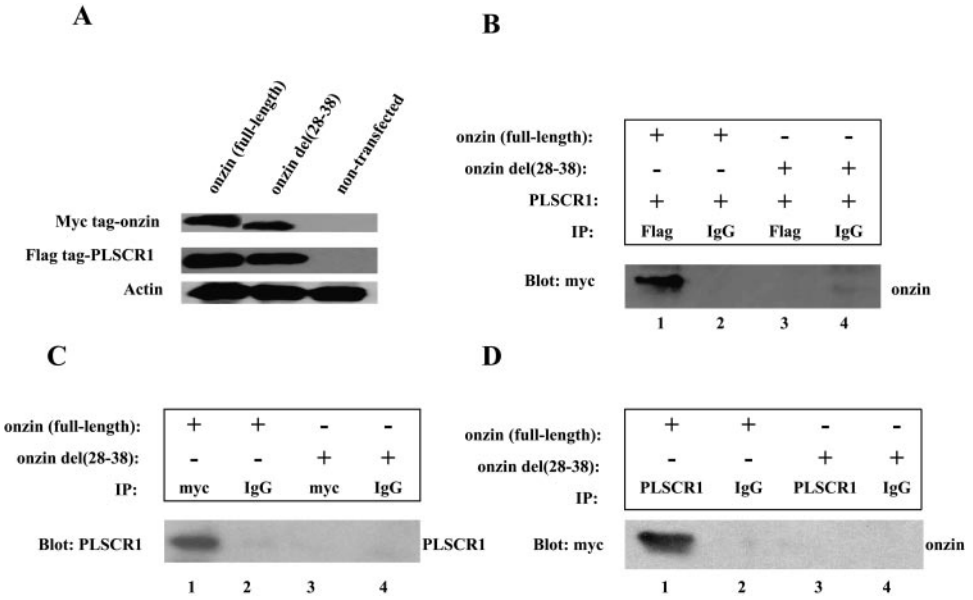

FIG. 4. Coimmunoprecipitation of onzin and PLSCR1 from Cos7 cells. (A) Myc epitope-tagged full-length murine onzin or the del28-38 mutant (Fig. 1) was coexpressed in Cos7 cells along with full-length human Flag epitope-tagged PLSCR1. Following lysis, each protein was detected by immunoblotting using antibodies specific for the indicated epitope tags. Blots were also probed with an antiactin monoclonal antibody as a control for protein loading. (B) The lysates from panel A were immunoprecipitated with the anti-Flag antibody or a control IgG. Precipitates were then immunoblotted and onzin protein was detected with the anti-Myc tag MAb. Note that the del28-38 onzin mutant did not interact with PLSCR1. (C) Myc epitope-tagged, onzin-overexpressing NIH 3T3 fibroblasts were generated by retroviral infection. Total lysates were then immunoprecipitated with a Myc epitope antibody or control IgG and blotted for associated endogenous PLSCR1. (D) The lysates in panel C were first precipitated with the anti-PLSCR1 MAb or control IgG. The blot was then probed with the anti-c-Myc MAb. Preliminary studies indicated that the cells expressed equivalent levels of wild-type and onzin(Δ28-38) protein (not shown).

munoprecipitation was specific was shown by the inability to precipitate onzin with control IgG (lane 2).

Finally, we asked whether endogenous PLSCR1 could be immunoprecipitated from cells that overexpressed onzin. For these experiments, we used NIH 3T3 murine fibroblasts, which express high levels of endogenous PLSCR1 (not shown). Following infection of these cells with a Myc epitope-tagged onzin-encoding retrovirus, either onzin (Fig. 4C) or PLSCR1 (Fig. 4D) was immunoprecipitated from total cell lysates and subjected to immunoblotting, with monoclonal antibodies directed against PLSCR1 or c-Myc, respectively. In the first case, immunoblotting demonstrated that onzin associated with endogenous PLSCR1, whereas in the second case, it was demonstrated that endogenous PLSCR1 was associated with onzin. In neither case was association between onzin(Δ28–38) and PLSCR1 demonstrated.

We conclude from this and the preceding studies that onzin and PLSCR1 colocalize and interact in both yeast and mammalian cells under a variety of conditions.

PLSCR1 reverses the antiapoptotic and proliferative properties of onzin. We have previously shown that the enforced expression of onzin in Rat1a fibroblasts markedly protects them from the proapoptotic consequences of serum deprivation or cytotoxic drug treatment (28). Moreover, these cells actually continue to proliferate, albeit at a somewhat reduced rate. To determine whether PLSCR affected these properties, we derived clonal isolates of Rat1a fibroblasts that expressed Myc-tagged PLSCR1, Myc-tagged onzin, or both proteins (Fig. 5A). Over 20 such clones of each type were identified, and most expressed their proteins at levels similar to those depicted here.

We next examined the consequences of two different apoptotic insults on the survival of each cell line. As shown in Fig. 5B, control Rat1a cells and those expressing only PLSCR1 showed similar survival patterns following the removal of serum or the addition of etoposide; in each case, >90% cell death occurred within 3 to 4 days. These findings are consistent with those of others showing that PLSCR1 overexpression per se does not necessarily impair cellular growth rate or induce apoptosis (30). In contrast, and as previously reported (28), cells expressing only onzin not only survived but continued to proliferate, whereas those which expressed both onzin and PLSCR1 showed a complete loss of onzin's protective effect. The ability of PLSCR1 to reverse onzin's positive effects on survival and proliferation was observed in several additional clones that were also examined (not shown).

Under standard conditions (10% fetal bovine serum), all cell lines grew at indistinguishable rates (not shown). However, at a limiting serum concentration (1% serum), onzin-expressing cells showed a significant growth advantage, whereas those expressing PLSCR1 and control cells grew at similar low rates (Fig. 5C). The coexpression of onzin and PLSCR1 resulted in a significant reduction in proliferation, indicating that the growth-promoting effects of onzin were blocked by PLSCR1.

We have previously shown that onzin overexpression increases the activity of the Akt1/protein kinase B oncoprotein, resulting in marked resistance of Rat1a cells to 6-thioguanine (28). This occurs with a frequency similar to that of cells with

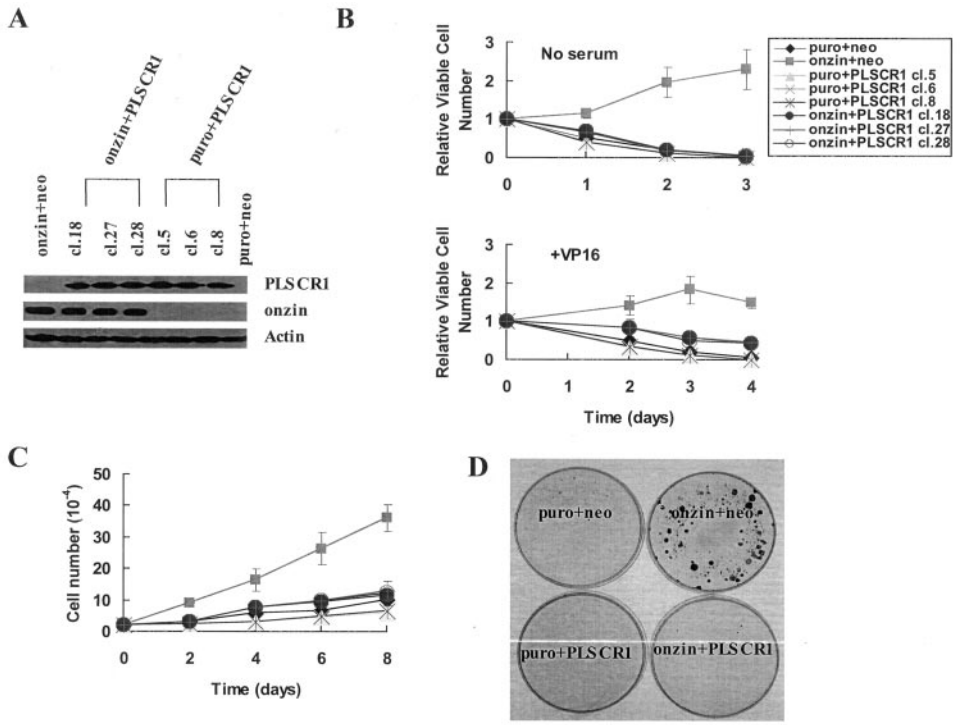

FIG. 5. PLSCR1 negates the proliferative and antiapoptotic phenotype conferred by onzin. (A) Rat1a cells were stably transfected with plasmids encoding Myc-tagged PLSCR1 and/or Myc-tagged onzin. Individual clones were then picked, expanded, and examined for the expression of each protein by immunoblotting (25 μg of protein/lane). Control blots for actin confirmed the presence of equivalent amounts of protein in each lane. (B) Equal numbers of cells from the indicated clones were seeded and then grown until approximately 50% confluence. They were then deprived of serum (top panel) or exposed continuously to 125 nM etoposide (bottom panel). Viable cells were then enumerated on successive days. Each point represents the average of triplicate determinations ± 1 standard error. (C) We plated 2×10^3 cells from the clones depicted in panel B in standard growth medium containing 1% fetal bovine serum. Total cell counts were then performed in triplicate at the indicated times and are depicted here as an average ± 1 standard error. Several additional clones expressing PLSCR1 at levels comparable to those depicted in panel A behaved similarly to the clones depicted here and in panel B (not shown). (D) Each of the indicated cell lines was seeded at 10^5 cells/plate and grown for 2 days, at which time the medium was changed and 6-thioguanine was added to a final concentration of 1 μM for 5 additional days. Plates were then stained with methylene blue as previously described (28). Very similar results were obtained with each of the clones shown in panel A (not shown).

defects in the mismatch repair mechanism and at >100 times the rate of spontaneous 6-thioguanine resistance, which typically involves mutation of the *HGPRT* gene (18). In order to determine whether PLSCR1 was affecting onzin through the latter protein's effects on Akt1 function, we examined the survival of representative cell lines over the course of continuous exposure to 1 μM 6-thioguanine. As shown in Fig. 5D and as previously reported (28), control Rat1a cells were highly sensitive to the drug, with virtually no surviving colonies observed at the completion of the experiment. In contrast, Rat1a-onzin cells showed significant 6-thioguanine resistance and formed numerous colonies of various sizes. Cells expressing PLSCR1 alone or in combination with onzin showed behavior identical to that of control cells. Thus, without affecting the intrinsic sensitivity of Rat1a cells, PLSCR1 markedly reversed the 6-thioguanine resistance of onzin-overexpressing cells.

Inhibition of endogenous PLSCR1 enhances the proliferation and apoptotic resistance of onzin-expressing cells. Onzin was initially characterized as a negative c-Myc target gene in 32D murine myeloid cells, which normally express high endogenous levels of onzin (25, 28). Down-regulation of onzin in these cells by shRNA results in a reduced rate of proliferation and increased sensitivity of apoptotic stimuli (28). Because 32D cells also express abundant PLSCR1 (Fig. 6A), we reasoned that its inhibition might enhance the activity of endogenous onzin and thus confer a proliferative advantage and antiapoptotic phenotype.

To test this hypothesis, we stably expressed a PLSCR1 shRNA in 32D cells and analyzed several of the resulting single-cell clones. As shown in Fig. 6A, each clone showed a >90% reduction in endogenous PLSCR1 protein compared to control cells. The former cells also proliferated more rapidly than control cells (Fig. 6B) and were significantly more resistant to apoptotic death following removal of the obligate hematopoietic cytokine IL-3 or upon exposure to the cytotoxic drug adriamycin (Fig. 6C and D). Similar results were seen in each of several additional PLSCR1-shRNA clones that expressed comparable reductions in PLSCR1 (not shown). In other studies we have shown that endogenous onzin transcript levels in clones expressing the PLSCR1 shRNA were identical to those of control cells and untransfected 32D cells (not shown). From these results, we conclude that the down-regulation of endogenous PLSCR1 in 32D cells is associated with phenotypes that mimic those seen with onzin overexpression.

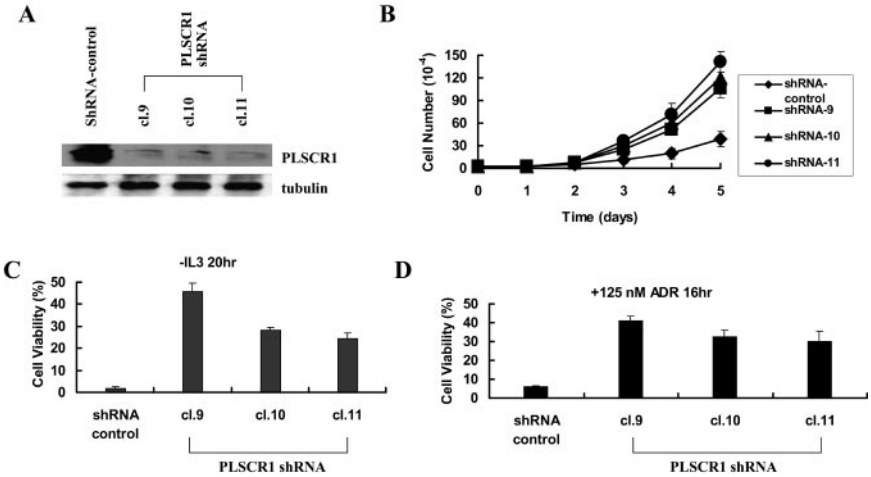

FIG. 6. shRNA-mediated knockdown of endogenous PLSCR1 in 32D myeloid cells enhances their proliferation and apoptotic resistance. (A) Endogenous PLSCR1 levels in clonal populations of 32D cells isolated following stable transfection with a control vector or with an shRNA vector targeting PLSCR1. Immunoblotting was performed using MAbs directed against PLSCR1 or tubulin as a control for protein loading. (B) Growth curves of 32D clones. Each of the indicated clones was seeded at a concentration of 2×10^3 cells/ml in standard RPMI growth medium supplemented with 10% fetal bovine serum and IL-3. On each subsequent day, the total number of cells/dish was counted in triplicate plates. Each point represents the average of these determinations ± 1 standard error. Similar behaviors were seen with several additional single-cell-derived clones (not shown). (C) Logarithmically growing 32D cells (>90% viability) were washed twice and replated in IL-3-deficient medium at a concentration of 5×10^5 cells/ml. Viability was then determined 20 h later on a Vi-Cell apparatus. A minimum of 2,000 cells were counted for each determination. The results shown represent the average percentage of viable cells from triplicate plates ± 1 standard error. (D) Cells were plated as described for panel C except that the medium contained IL-3 plus 125 nM adriamycin (ADR). Cell viability was determined as described for panel C.

Minimal domain of PLSCR1 interacts with onzin and reverses its proliferative and antiapoptotic phenotype. Our previous and current studies indicated that the small, cysteine-rich region of onzin encompassing residues 28 to 38 interacted with PLSCR1 and was necessary for onzin's biological activities (Fig. 1 and 4) (28). Additionally, our initial yeast two-hybrid studies indirectly suggested that the region of human PLSCR1 that interacted with onzin includes resides from ca. 160 to 250 (Fig. 2B).

In order to examine the putative onzin-interacting domain of PLSCR1 more definitively, we derived several single-cell clones of Rat1a-onzin fibroblasts that stably expressed amino acids 160 to 250 of PLSCR1 as a Myc epitope-tagged protein. As a negative control, we derived Rat1a-onzin clones expressing the Myc epitope-tagged 1 to 163 region of PLSCR1. As a further control set, we also established Rat1a cells that expressed each of the above PLSCR1 proteins. As shown in Fig. 7A, all of the clones chosen for further study expressed equivalent levels of their PLSCR1 proteins.

We next asked whether, as previously demonstrated for full-length PLSCR1 (Fig. 4B), the truncated PLSCR1 proteins also associated with onzin. Lysates from cells expressing these proteins were therefore precipitated with anti-PLSCR1 or control MAbs and subjected to immunoblotting with the anti-Myc tag MAb. As shown in Fig. 7B, onzin was detected in association with PLSCR1(160–250) but not in association with PLSCR1(1–163). Together with our original yeast two-hybrid observations, these results unequivocally establish that the region encompassing amino acids 160 to 250 of PLSCR1 comprises its onzin-interacting domain.

We then asked whether the expression of this minimal PLSCR1 domain was sufficient to reverse onzin's positive effects on survival and proliferation. As shown in Fig. 8A and B,

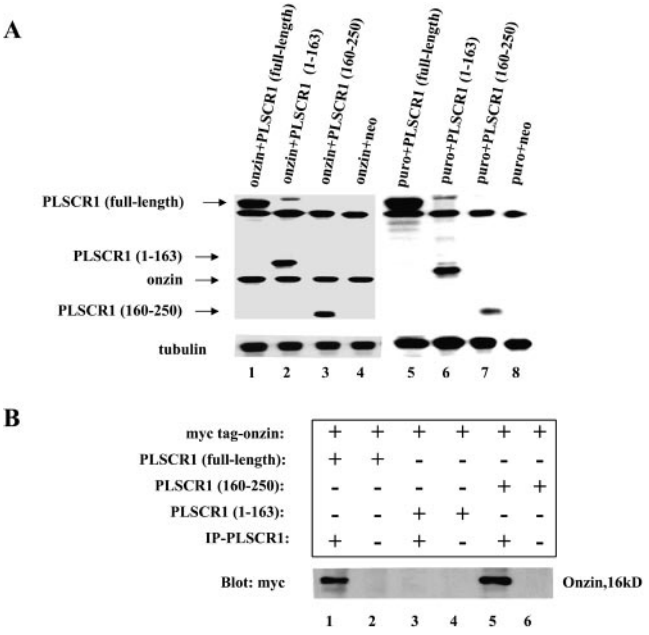

FIG. 7. Region between amino acids 160 and 250 of PLSCR1 is required for its interaction with and inhibition of onzin. (A) Individual Rat1a-onzin clones (lanes 1 to 4) or control Rat1a-puro clones (lanes 5 to 8) expressing full-length PLSCR1, PLSCR1(160–250), or PLSCR1(1–163) were subjected to immunoblotting. Both onzin and PLSCR1 proteins were Myc epitope tagged and thus were detected simultaneously with the 9E10 anti-Myc MAb. (B) Coimmunoprecipitation of onzin and full-length PLSCR1 and PLSCR1(160–250). The Rat1a cell lines shown in panel A were lysed, immunoprecipitated with anti-PLSCR1 MAb and immunoblotted using the 9E10 anti-Myc MAb. + and − indicate the expression or lack thereof of the indicated proteins based on the immunoblot analysis depicted in panel A. Note that onzin coimmunoprecipitated with full-length PLSCR1 and PLSCR1(160–250) but not with PLSCR1(1–163).

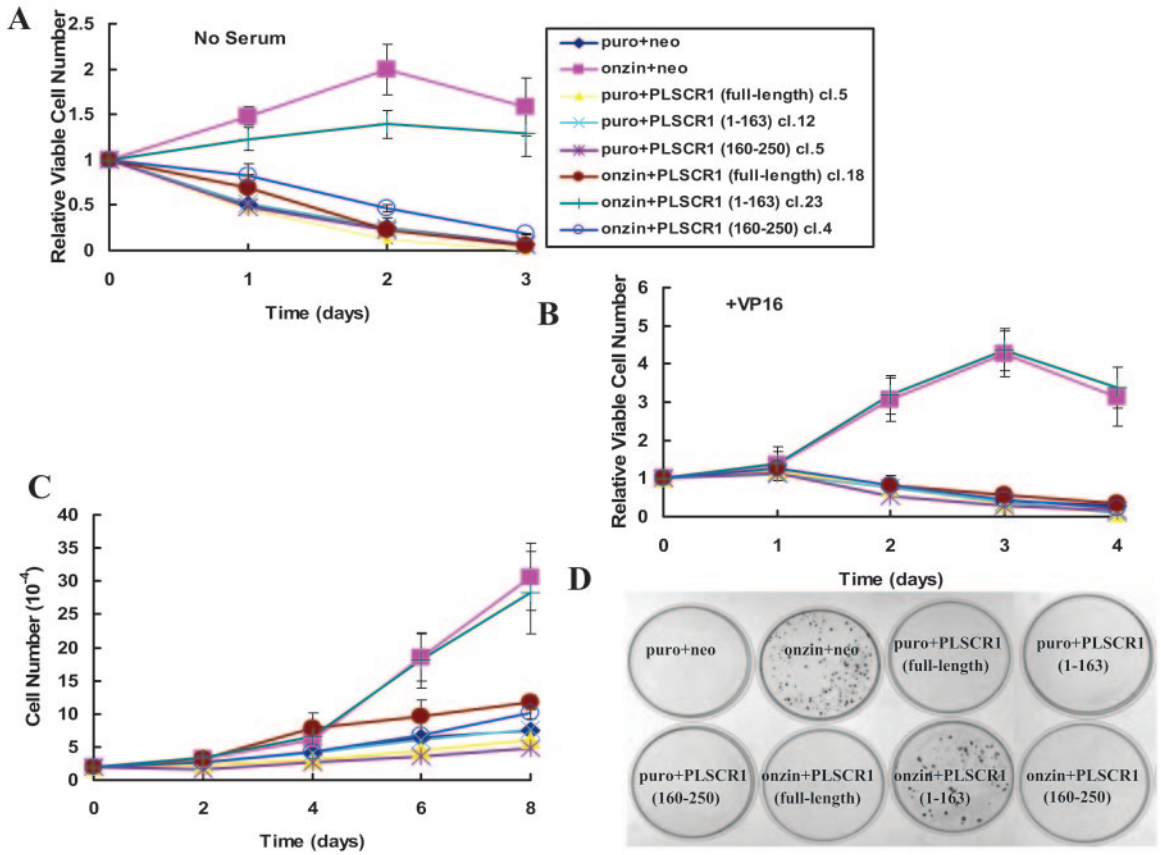

FIG. 8. Domain from 160 to 250 of PLSCR1 is sufficient to inhibit onzin's biological effects. (A) Each of the clones described in the legend to Fig. 7 was grown to approximately 50% confluence and deprived of serum, and the residual viable cells were quantified on a daily basis. (B) Cells were grown as described for panel A except that fresh medium containing 125 nM etoposide (VP16) was added on day 0. Residual viable cells were quantified on subsequent days. (C) Cells were seeded at equivalent low densities (2×10^3 cells/well) in medium containing 1% fetal calf serum. Subsequent cell counts were performed at the indicated times. In panels A to C, all points represent the average of triplicate determinations ± 1 standard error. (D) Each of the indicated clones was seeded as described in the legend to Fig. 5D and subsequently incubated in medium containing 1 μM 6-thioguanine. Methylene blue-stained colonies were then visualized on days 5 and 6.

Rat1a-onzin cells showed the expected marked resistance to both serum withdrawal and etoposide treatment, confirming our previous findings (Fig. 5) (28). However, when these cells were subsequently forced to express either full-length PLSCR1 or PLSCR1(160–250), they reverted to their original, highly sensitive phenotype. In contrast, this property was noticeably absent in cells which expressed PLSCR1(1–163). Consistent with our previous observations (Fig. 5), none of the PLSCR1 proteins, when expressed alone, affected the behavior of Rat1a cells. Similarly, both full-length PLSCR1 and PLSCR1(160–250) but not PLSCR1(1–163) were able to inhibit the growth of Rat1a-onzin cells maintained in 1% serum (Fig. 8C). Finally, both full-length PLSCR1 and PLSCR1(160–250) were able to reverse the 6-thioguanine resistance of Rat1a-onzin cells (Fig. 8D), whereas PLSCR1(1–163) was completely ineffective.

Taken together, these studies confirm that PLSCR1's interaction with and functional antagonism to onzin maps to a 90-amino-acid domain of PLSCR1 and that this segment is both necessary and sufficient for these functions.

PLSCR1 prevents onzin's association with and activation of Akt1 and Mdm2. We have previously shown that onzin's ability to confer a survival and proliferative advantage on Rat1a fibroblasts correlates with its association with and phosphorylation-dependent activation of Akt1 and Mdm2 (28). Activation of Akt1 is also consistent with the marked resistance of onzin-expressing fibroblasts to 6-thioguanine (Fig. 5D and 8D) (28). Therefore, to determine whether the mechanism of action of PLSCR1 involved its interference with onzin's interaction with Akt1 and Mdm2, we first performed coimmunoprecipitations with representative Rat1a cell lines, as shown in Fig. 8. As shown in Fig. 9A, both Akt1 and Mdm2 associated with onzin in control cells (lane 2) and in cells overexpressing the biologically inactive PLSCR1(1–163) deletion. However, this association was not detected in cells expressing full-length PLSCR1 or the active PLSCR1(160–250) mutant.

We next exposed the above-described cell lines to 125 nM etoposide and then assessed the levels of total Akt1, Akt1 phosphorylated on Ser473 (pAkt), total Mdm2, and Mdm2 phosphorylated on Ser166 (pMdm2) by immunoblotting at daily intervals thereafter (Fig. 9B). As previously shown (28), total Akt1 and Mdm2 levels remained relatively constant in all cell lines over the course of the experiment. However, the levels of both pAkt and pMdm2 declined significantly in control cells following the addition of etoposide (Fig. 9B, row 1).

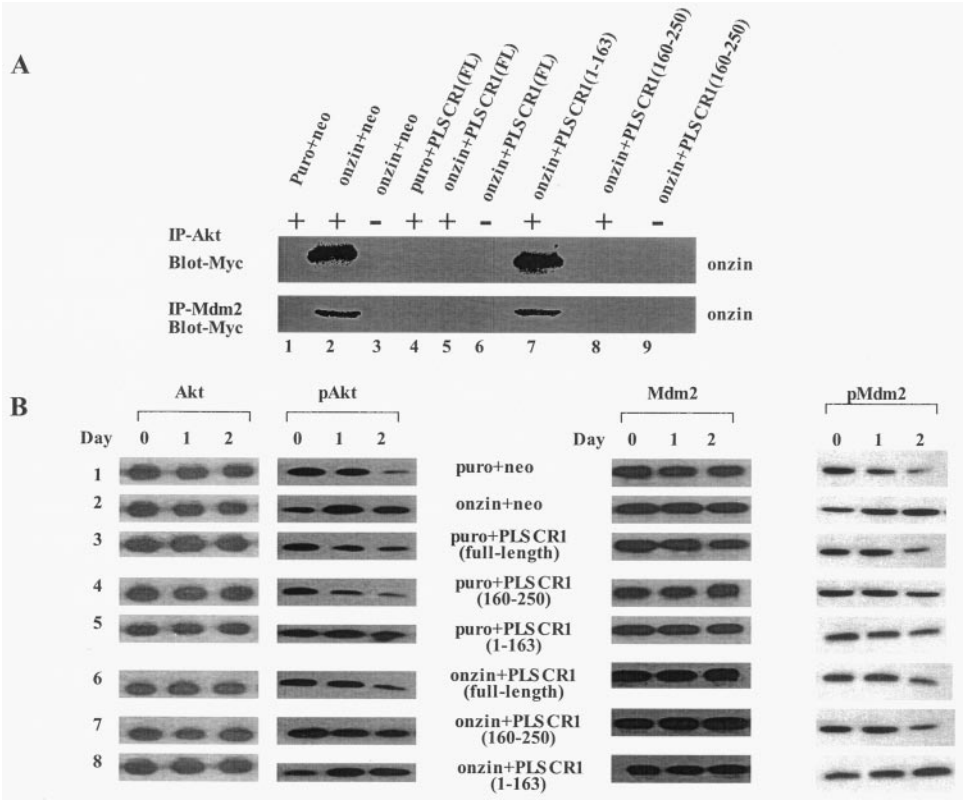

FIG. 9. PLSCR1 inhibits onzin's ability to interact with and regulate Akt1 and Mdm2. (A) Coimmunoprecipitation experiments demonstrating the association between onzin and Akt1 and Mdm2 and its reversal by PLSCR1. The indicated cell lines were lysed and immunoprecipitated with antibodies to either Akt1 or Mdm2 (+) or with a control IgG (−) as previously described (28). Immunoblotting was then performed on the precipitates with an anti-Myc monoclonal antibody to detect Myc epitope-tagged onzin. (B) PLSCR1 overexpression blocks onzin's ability to promote phosphorylation-dependent activation of Akt1 and Mdm2. Each of the indicated cell lines was exposed to 125 nM etoposide for the indicated times. After lysis, 50 μg of total lysate from each time point was then subjected to immunoblotting for the indicated proteins or phosphoproteins. In other experiments, blots were stripped and reprobed with an antitubulin MAb to confirm the loading of equivalent amounts of total lysate (see Fig. 10). In the case of pAkt1, day 0 and day 2 ratios of proteins were compared by densitometric scanning and were typical of several independent experiments. These ratios ranged from 1.2 to 2.3 for rows 1, 3, 4, 5, 6, and 7 and were 0.7 and 0.5 for rows 2 and 8, respectively.

In contrast, and also as previously reported (28), the levels of these phosphoproteins either remained constant or increased in onzin-overexpressing cells (Fig. 9B, row 2). In keeping with their indistinguishable biological behaviors (Fig. 5), Rat1a cells that expressed all forms of PLSCR1 modulated their levels of pAkt and pMdm2 in a manner similar to that seen in control cells (Fig. 9B, rows 3 to 5). Finally, and most importantly, cells overexpressing both onzin and either full-length PLSCR1 or the biologically active 160 to 250 region of PLSCR1 showed a down-regulation of phosphoprotein levels (Fig. 9B, rows 6 and 7), whereas no such down-regulation was observed in cells expressing onzin and the biologically inert PLSCR1(1–163) protein (Fig. 9B, row 8). Together with the results presented in Fig. 8A, those presented here indicate that PLSCR1 competes with Akt1 and Mdm2 for binding to onzin and that, in doing so, it reverses onzin's positive effects on Akt1 and Mdm2 phosphorylation and, ultimately, on survival and proliferation.

Reversal of the onzin phenotype by PLSCR1 involves renormalization of the p53 response. Our previous studies, as well as those presented above, have demonstrated that onzin's ability to promote proliferation and survival coincides with a phosphorylation-dependent activation of Akt1 and Mdm2, ultimately leading to marked loss of both p53 expression and sustained G_2/M checkpoint arrest (28). According to this model, blocking the actions of onzin by PLSCR1 should restore p53 inducibility and cell cycle arrest in response to apoptotic stimuli. As shown in Fig. 10A and as previously demonstrated (28), control Rat1a cells exposed to etoposide showed a time-dependent induction of p53, whereas Rat1a-onzin cells actually showed a decrease in p53 (Fig. 10A, compare rows 1 and 2). Consistent with their Rat1a-like phenotype, Rat1a-PLSCR1 cells, Rat1a-PLSCR1(1–163) cells, and Rat1a-PLACR1(160–250) cells also showed significant induction of p53 (Fig. 10A, rows 3 to 5). A similar up-regulation of p53 was seen in Rat1a-onzin cells which expressed either full-length PLSCR1 or PLSCR1(160–250) (Fig. 10A, rows 6 and 7) but not in Rat1a-onzin cells expressing PLSCR1(1–163) (Fig. 10A, row 8).

All Rat1a cell lines that were able to up-regulate p53 also showed a marked and sustained G_2/M arrest and the eventual appearance of subdiploid apoptotic cells (Fig. 10B). However, when p53 was not induced, the G_2/M arrest was transient and was associated with an accumulation of cells in the G_0/G_1 phase of the cell cycle (Fig. 10B, rows 2 and 8). These cell cycle

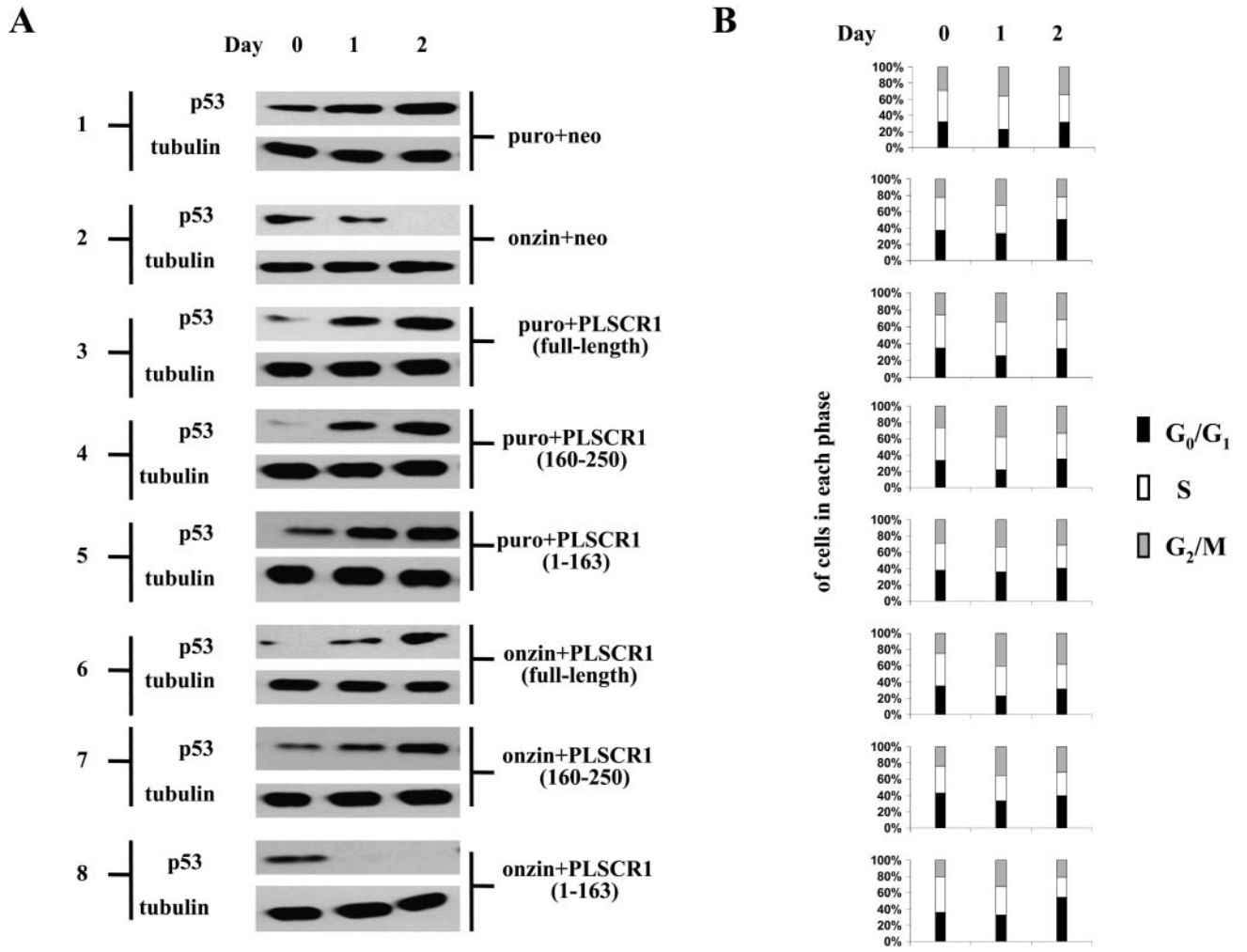

FIG. 10. PLSCR1 reverses onzin's ability to suppress p53 induction and G_2/M arrest. (A) The lysates in Fig. 9B were used to detect total p53 protein. As a control for protein loading, tubulin was also detected in each sample. (B) At the time of cell harvest shown in panel A, a separate aliquot of cells was stained with propidium iodide and subjected to flow cytometry to quantify the fraction of each cell population in G_0/G_1, S, and G_2/M. The numbers indicate the averages of triplicate determinations, and each figure displays a typical determination for that sample.

changes coincided with the continued, albeit slowed, growth and increased survival of the cell lines (Fig. 5B). These results indicate that the interaction between onzin and the onzin-interacting domain of PLSCR1 results in the predicted renewed capacity to induce p53 and undergo cell cycle arrest and apoptosis in response to appropriate stimuli.

DISCUSSION

We have previously demonstrated in myeloid cells that ectopic c-Myc expression coincides with a marked reduction in endogenous onzin levels and increased susceptibility to apoptotic stimuli (25, 28). That the down-regulation of onzin is causally related to this phenotype was demonstrated by knocking down endogenous onzin with stably expressed shRNA. Despite the fact that these cells contained normal levels of c-Myc, they proliferated more slowly and were hypersensitive to apoptotic stimuli compared to cells with normal onzin levels. Furthermore, these properties could be reversed by the enforced expression of an shRNA-resistant form of onzin. Conversely, the overexpression of onzin in Rat1a fibroblasts, which do not normally express the protein, was sufficient to inhibit apoptosis, to enhance growth, and to transform. These experiments support the idea that, at least in cells in which it is normally expressed, onzin plays a central role in the regulation of c-Myc-mediated apoptosis. However, other pathways, both p53 dependent and p53 independent, are also important for the full expression of this phenotype (27). This is underscored by the observation that the properties imparted by onzin appear to occur as a result of its interaction with and activation of the Akt1 and Mdm2 oncoproteins, both of which are also regulated at other levels by c-Myc (Fig. 9) (16, 17, 45). Together, these responses lead to a suppression of p53 induction and a loss of G_2/M arrest by onzin-overexpressing cells in the face of apoptotic stimuli.

The current finding that onzin also interacts with and is inhibited by PLSCR1 is consistent with several of the known functions of the latter protein. For example, several studies

have linked PLSCR1 overexpression with reduced proliferation, enhanced apoptosis, and less-aggressive tumor behavior (30, 41). PLSCR$^{-/-}$ mice show impaired granulocytic differentiation and reduced sensitivity to hematopoietic cytokines such as stem cell factor and granulocyte colony-stimulating factor (43). PLSCR1 has been reported to interact with a variety of growth factor signaling intermediates, including c-Src, protein kinase Cδ, c-Abl, Shc, and the epidermal growth factor receptor, and to be a substrate for the first three kinases (23, 32). Thus, rather than playing a strictly promotional role in growth inhibition and apoptosis, the true function of PLSCR1 may be to integrate and interpret both stimulatory and inhibitory signals pertaining to proliferation and apoptosis.

The results reported here provide a potential link between the nuclear transcription factor c-Myc and apoptosis-related phospholipid remodeling at the cell surface. Aminophospholipids such as phosphatidylserine are normally maintained, via an ATP-dependent-lipid transporter mechanism, in an asymmetric conformation, embedded within the inner leaflet of the plasma membrane. The externalization of phosphatidylserine is believed to be one of the cardinal signals for apoptotic cell recognition and engulfment by the phagocytic system (3, 34). In addition to its putative role in mediating cell surface exposure to phosphatidylserine, PLSCR1 has also been proposed to play a more proximal and direct role in the actual induction of apoptosis, as evidenced by the fact that apoptosis can be induced by PLSCR1 overexpression in vitro, leading to reduced growth and increased cell surface expression of phosphatidylserine (2, 41).

We have previously shown that onzin physically interacts with and modifies the activities of the serine/threonine kinase Akt1 and the Akt1 substrate Mdm2 (28). These findings suggest that onzin's role in promoting proliferation, enhancing survival, and overcoming cell cycle arrest involves its ability to control the activities of two key upstream regulators of the p53 tumor suppressor. We propose that PLSCR1, by also interacting with onzin, serves as a negative, albeit indirect, regulator of these activities. Our findings that onzin and PLSCR1 colocalize in a pattern that is strikingly similar to that of Akt1 and Mdm2 also supports this idea (Fig. 3). It will be of interest in future work to determine whether the intimate physical relationships of these proteins is also associated with functional alterations.

In conclusion, we have shown here that onzin interacts with and is inhibited by PLSCR1, thus providing a means by which the promotion of apoptosis by c-Myc can be positively influenced at its earliest stages. This complements more-distal and c-Myc-independent effects of PLSCR1 on apoptosis that involve its originally described role in the maintenance of plasma membrane phospholipid symmetry. This novel relationship reveals a contiguous functional link between the earliest events mediated by c-Myc and the latest ones, which culminate at the cell surface and lead to phospholipid reshuffling and cell death.

ACKNOWLEDGMENTS

We thank Elaine Fernandes for DNA sequencing and Kristi Rothermund for advice on fluorescence microscopy.

This work was supported by NIH grants CA078259 and CA105033 to E.V.P., NIH grants HL36946 and HL63819 to P.J.S., and a postdoctoral fellowship award from the Research Advisory Committee of Children's Hospital of Pittsburgh to Y.L.

REFERENCES

1. **Arabi, A., S. Wu, K. Ridderstrale, H. Bierhoff, C. Shiue, K. Fatyol, S. Fahlen, P. Hydbring, O. Soderberg, I. Grummt, L. G. Larsson, and A. P. Wright.** 2005. c-Myc associates with ribosomal DNA and activates RNA polymerase I transcription. Nat. Cell Biol. **7:**303–310.
2. **Bailey, K., H. W. Cook, and C. R. McMaster.** 2005. The phospholipid scramblase PLSCR1 increases UV induced apoptosis primarily through the augmentation of the intrinsic apoptotic pathway and independent of direct phosphorylation by protein kinase C delta. Biochim. Biophys. Acta **1733:** 199–209.
3. **Balasubramanian, K., and A. J. Schroit.** 2003. Aminophospholipid asymmetry: a matter of life and death. Annu. Rev. Physiol. **65:**701–734.
4. **Ben-Efraim, I., Q. Zhou, T. Wiedmer, L. Gerace, and P. J. Sims.** 2004. Phospholipid scramblase 1 is imported into the nucleus by a receptor-mediated pathway and interacts with DNA. Biochemistry **43:**3518–3526.
5. **Bevers, E. M., P. Comfurius, D. W. Dekkers, and R. F. Zwaal.** 1999. Lipid translocation across the plasma membrane of mammalian cells. Biochim. Biophys. Acta **1439:**317–330.
6. **Braspenning, J., A. Marchini, V. Albarani, L. Levy, F. Ciccolini, C. Cremonesi, R. Ralston, L. Gissmann, and M. Tommasino.** 1998. The CXXC Zn binding motifs of the human papillomavirus type 16 E7 oncoprotein are not required for its in vitro transforming activity in rodent cells. Oncogene **16:**1085–1089.
7. **Chen, M. H., I. Ben-Efraim, G. Mitrousis, N. Walker-Kopp, P. J. Sims, and G. Cingolani.** 2005. Phospholipid scramblase 1 contains a nonclassical nuclear localization signal with unique binding site in importin alpha. J. Biol. Chem. **280:**10599–10606.
8. **Chivers, P. T., M. C. Laboissiere, and R. T. Raines.** 1996. The CXXC motif: imperatives for the formation of native disulfide bonds in the cell. EMBO J. **15:**2659–2667.
9. **Chivers, P. T., K. E. Prehoda, and R. T. Raines.** 1997. The CXXC motif: a rheostat in the active site. Biochemistry **36:**4061–4066.
10. **Coller, H. A., C. Grandori, P. Tamayo, T. Colbert, E. S. Lander, R. N. Eisenman, and T. R. Golub.** 2000. Expression analysis with oligonucleotide microarrays reveals that MYC regulates genes involved in growth, cell cycle, signaling, and adhesion. Proc. Natl. Acad. Sci. USA **97:**3260–3265.
11. **Collet, J. F., J. C. D'Souza, U. Jakob, and J. C. Bardwell.** 2003. Thioredoxin 2, an oxidative stress-induced protein, contains a high affinity zinc binding site. J. Biol. Chem. **278:**45325–45432.
12. **Fadeel, B., B. Gleiss, K. Hogstrand, J. Chandra, T. Wiedmer, P. J. Sims, J. L. Henter, S. Orrenius, and A. Samali.** 1999. Phosphatidylserine exposure during apoptosis is a cell-type-specific event and does not correlate with plasma membrane phospholipid scramblase expression. Biochem. Biophys. Res. Commun. **266:**504–511.
13. **Fernandez, P. C., S. R. Frank, L. Wang, M. Schroeder, S. Liu, J. Greene, A. Cocito, and B. Amati.** 2003. Genomic targets of the human c-Myc protein. Genes Dev. **17:**1115–1129.
14. **Fomenko, D. E., and V. N. Gladyshev.** 2003. Identity and functions of CxxC-derived motifs. Biochemistry **42:**11214–11225.
15. **Grandori, C., N. Gomez-Roman, Z. A. Felton-Edkins, C. Ngouenet, D. A. Galloway, R. N. Eisenman, and R. J. White.** 2005. c-Myc binds to human ribosomal DNA and stimulates transcription of rRNA genes by RNA polymerase I. Nat. Cell Biol. **7:**311–318. (Erratum, **7:**531.)
16. **Guo, Q. M., R. L. Malek, S. Kim, C. Chiao, M. He, M. Ruffy, K. Sanka, N. H. Lee, C. V. Dang, and E. T. Liu.** 2000. Identification of c-myc responsive genes using rat cDNA microarray. Proc. Natl. Acad. Sci. USA **60:**5922–5928.
17. **Jacobs, J. J., B. Scheijen, J. W. Voncken, K. Kieboom, A. Berns, and M. van Lohuizen.** 1999. Bmi-1 collaborates with c-Myc in tumorigenesis by inhibiting c-Myc-induced apoptosis via INK4a/ARF. Genes Dev. **13:**2678–2690.
18. **Kandel, E. S., J. Skeen, N. Majewski, A. DiCristofano, P. P. Pandolfi, C. S. Feliciano, A. Gartel, and N. Hay.** 2002. Activation of Akt/protein kinase B overcomes a G_2/M cell cycle checkpoint induced by DNA damage. Mol. Cell. Biol. **22:**7831–7841.
19. **Landay, M., S. K. Oster, F. Khosravi, L. E. Grove, X. Yin, J. Sedivy, L. Z. Penn, and E. V. Prochownik.** 2000. Promotion of growth and apoptosis in c-myc nullizygous fibroblasts by other members of the myc oncoprotein family. Cell Death Differ. **7:**697–705.
20. **Langlands, K., X. Yin, G. Anand, and E. V. Prochownik.** 1997. Differential interactions of Id proteins with basic-helix-loop-helix transcription factors. J. Biol. Chem. **272:**19785–19793.
21. **Langlands, K., and E. V. Prochownik.** 1997. A rapid method for the preparation of yeast lysates that facilitates the immunodetection of proteins generated by the yeast two-hybrid system. Anal. Biochem. **249:**250–252.
22. **Mu, Z. M., X. Y. Yin, and E. V. Prochownik.** 2002. Pag, a putative tumor suppressor, interacts with the Myc Box II domain of c-Myc and selectively alters its biological function and target gene expression. J. Biol. Chem. **277:**43175–43184.
23. **Nanjundan, M., J. Sun, J. Zhao, Q. Zhou, P. J. Sims, and T. Wiedmer.** 2003. Plasma membrane phospholipid scramblase 1 promotes EGF-dependent activation of c-Src through the epidermal growth factor receptor. J. Biol. Chem. **278:**37413–37418.

24. **Nesbit, C. E., J. M. Tersak, and E. V. Prochownik.** 1999. MYC oncogenes and human neoplastic disease. Oncogene **18:**3004–3016.
25. **Nesbit, C. E., J. M. Tersak, L. E. Grove, A. Drzal, H. Choi, and E. V. Prochownik.** 2000. Genetic dissection of c-myc apoptotic pathways. Oncogene **19:**3200–3212.
26. **Packham, G., and J. L. Cleveland.** 1995. The role of ornithine decarboxylase in c-Myc-induced apoptosis. Curr. Top. Microbiol. Immunol. **194:**283–290.
27. **Prendergast, G. C.** 1999. Mechanisms of apoptosis by c-Myc. Oncogene **18:**2967–2987.
28. **Rogulski, K., Y. Li, K. Rothermund, L. Pu, Watkins, S. Yi, and E. V. Prochownik.** 2005. Onzin, a c-Myc-repressed target, promotes survival and transformation by modulating the Akt-Mdm2-p53 pathway. Oncogene **24:** 7524–7541.
29. **Rothermund, K., K. Rogulski, E. Fernandes, A. Whiting, J. Sedivy, L. Pu, and E. V. Prochownik.** 2005. C-Myc-independent restoration of multiple phenotypes by two C-Myc target genes with overlapping functions. Cancer Res. **65:**2097–2107.
30. **Silverman, R. H., A. Halloum, A. Zhou, B. Dong, F. Al-Zoghaibi, D. Kushner, Q. Zhou, J. Zhao, T. Wiedmer, and P. J. Sims.** 2002. Suppression of ovarian carcinoma cell growth in vivo by the interferon-inducible plasma membrane protein, phospholipid scramblase 1. Cancer Res. **62:**397–402.
31. **Sims, P. J., and T. Wiedmer.** 2001. Unraveling the mysteries of phospholipid scrambling. Thromb. Haemostasis. **86:**266–275.
32. **Sun, J., J. Zhao, M. A. Schwartz, J. Y. Wang, T. Wiedmer, and P. J. Sims.** 2001. c-Abl tyrosine kinase binds and phosphorylates phospholipid scramblase 1. J. Biol. Chem. **276:**28984–28990.
33. **Sun, J., M. Nanjundan, L. J. Pike, T. Wiedmer, and P. J. Sims.** 2002. Plasma membrane phospholipid scramblase 1 is enriched in lipid rafts and interacts with the epidermal growth factor receptor. Biochemistry **41:**6338–6345.
34. **Vance, J. E.** 2003. Molecular and cell biology of phosphatidylserine and phosphatidylethanolamine metabolism. Progress Nucleic Acid Res. Mol. Biol. **75:**69–111.
35. **White R. J.** 2005. RNA polymerases I and III, growth control and cancer. Nat. Rev. Mol. Cell Biol. **6:**69–78.
36. **Wiedmer, T., J. Zhaom, M. Nanjundanm, and P. J. Sims.** 2003. Palmitoylation of phospholipid scramblase 1 controls its distribution between nucleus and plasma membrane. Biochemistry **42:**1227–1233.
37. **Xu, Y., T. F. Sumter, R. Bhattacharya, A. Tesfaye, E. J. Fuchs, L. J. Wood, D. L. Huso, and L. M. Resar.** 2004. The HMG-I oncogene causes highly penetrant, aggressive lymphoid malignancy in transgenic mice and is overexpressed in human leukemia. Cancer Res. **64:**3371–3375.
38. **Yin, X. Y., K. Gupta, W. P. Han, E. S. Levitan, and E. V. Prochownik.** 1999. Mmip-2, a novel RING finger protein that interacts with mad members of the Myc oncoprotein network. Oncogene **18:**6621–6634.
39. **Yin, X., M. F. Landay, W. Han, E. S. Levitan, S. C. Watkins, R. M. Levenson, D. L. Farkas, and E. V. Prochownik.** 2001. Dynamic in vivo interactions among Myc network members. Oncogene **20:**4650–4664.
40. **Yin, X., L. Grove, K. Rogulski, and E. V. Prochownik.** 2002. Myc target in myeloid cells-1, a novel c-Myc target, recapitulates multiple c-Myc phenotypes. J. Biol. Chem. **277:**19998–20010.
41. **Yu, A., C. R. McMaster, D. M. Byers, N. D. Ridgway, and H. W. Cook.** 2003. Stimulation of phosphatidylserine biosynthesis and facilitation of UV-induced apoptosis in Chinese hamster ovary cells overexpressing phospholipid scramblase 1. J. Biol. Chem. **278:**9706–9714.
42. **Zhou, Q., P. J. Sims, and T. Wiedmer.** 1998. Expression of proteins controlling transbilayer movement of plasma membrane phospholipids in the B lymphocytes from a patient with Scott syndrome. Biochemistry **37:**2356–2360.
43. **Zhou, Q., J. Zhao, T. Wiedmer, and P. J. Sims.** 2002. Normal hemostasis but defective hematopoietic response to growth factors in mice deficient in phospholipid scramblase 1. Blood **99:**4030–4038.
44. **Zhou, Q., I. Ben-Efraim, J.-L. Bigcas, T. Wiedmer, and P. J. Sims.** 2005. Phospholipid scramblase 1 binds to the promoter region of the inositol 1,4,5-triphosphate receptor type 1 gene to enhance its expression. J. Biol. Chem. **280:**35062–35068.
45. **Zindy, F., C. M. Eischen, D. H. Randle, T. Kamijo, J. L. Cleveland, C. J. Sherr, and M. F. Roussel.** 1998. Myc signaling via the ARF tumor suppressor regulates p53-dependent apoptosis and immortalization. Genes Dev. **12:** 2424–2433.